JOURNAL OF GEOPHYSICAL RESEARCH, VOL. 104, NO. D16, PAGES 19,705–19,721, AUGUST 27, 1999

A space-time downscaling model for rainfall

V. Venugopal[1], Efi Foufoula-Georgiou, and Victor Sapozhnikov

St. Anthony Falls Laboratory, Department of Civil Engineering, University of Minnesota, Minneapolis

Abstract. Interpretation of the impact of climate change or climate variability on water resources management requires information at scales much smaller than the current resolution of regional climate models. Subgrid-scale variability of precipitation is typically resolved by running nested or variable resolution models or by statistical downscaling, the latter being especially attractive in ensemble predictions due to its computational efficiency. Most existing precipitation downscaling schemes are based on spatial disaggregation of rainfall patterns, independently at different times, and do not properly account for the temporal persistence of rainfall at the subgrid spatial scales. Such a temporal persistence in rainfall directly relates to the spatial variability of accumulated local soil moisture and might be important if the downscaled values were to be used in a coupled atmospheric-hydrologic model. In this paper we propose a rainfall downscaling model which utilizes the presence of dynamic scaling in rainfall [*Venugopal et al.*, 1999] and which in conjunction with a spatial disaggregation scheme preserves both the temporal and spatial correlation structure of rainfall at the subgrid scales.

1. Introduction

Interpretation of the impact of climate variability on water resources management requires information at scales much smaller than the current resolution of regional or global climate models. Subgrid-scale variability of precipitation is typically resolved (1) by running nested or variable resolution models or (2) by statistical downscaling. The schemes that fall in the former category are often unattractive for mainly two reasons: (1) Running physical models at very fine resolutions is computationally prohibitive, and (2) the physics at small scales is often not understood or parameterized well, and merely increasing the model resolution without explicitly resolving the small-scale physics in the model does not necessarily produce more accurate predictions. On the other hand, the schemes from the latter framework, namely, statistical schemes, are computationally efficient and especially attractive in ensemble predictions due to their simplicity.

The existing statistical precipitation downscaling schemes have, in turn, their own deficiencies (e.g., see *Wilby et al.* [1997] for a review of some schemes and their limitations). Most are based on spatial disaggregation of rainfall patterns, independently at different instants of time, and thus they do not properly account for the temporal persistence of rainfall at the subgrid spatial scales. Such a temporal persistence in rainfall directly relates to the spatial variability of accumulated local soil moisture and might be important if the downscaled values were to be used in a coupled atmospheric-hydrologic model. Another limitation of most schemes is that they are scale-dependent, and thus new parameterizations are needed every time the desired scale of downscaling changes. In this work, we present a downscaling model which does not suffer from any of the above limitations; that is, it is scale-invariant and preserves both the spatial and temporal correlation structure of rainfall at the subgrid scales.

Many studies have indicated the presence of scale-invariance in spatial and/or temporal rainfall [*Gupta and Waymire*, 1990; *Schertzer and Lovejoy*, 1987; *Kumar and Foufoula-Georgiou*, 1993; *Olsson et al.*, 1993; *Veneziano et al.*, 1996]. In a recent study, *Venugopal et al.* [1999] analyzed spatial and temporal rainfall patterns simultaneously and found the presence of a type of space-time scale invariance, namely, dynamic scaling. Specifically, they found that the rate of evolution of rainfall remains invariant under space-time transformations of the form $t \sim L^z$; that is, the dependence of rainfall on time (t) and space (L) can be reduced to a single parameter t/L^z. The space-time downscaling model that we propose utilizes the unraveled spatio-temporal organization in introducing temporal persistence into downscaling.

[1]Now at Center for Ocean-Land-Atmosphere Studies, Maryland.

Paper number 1999JD900338.
0148-0227/99/1999JD900338$09.00

The structure of the present paper is as follows: In section 2, we briefly summarize the basic hypotheses on which we built our model, namely, the simple scaling relationships in spatial rainfall fluctuations and the spatiotemporal organization that was found in rainfall. In section 3, we propose a downscaling model which in conjunction with the spatial disaggregation scheme of *Perica and Foufoula-Georgiou* [1996b] helps introduce temporal persistence into subgrid-scale spatial rainfall. Section 4 presents the implementation of the space-time downscaling model on actual rainfall fields. Section 5 evaluates the model performance, and finally, concluding remarks along with ideas for future research are presented in section 6.

2. Review of Scaling Relationships in Rainfall

2.1. Summary of Simple Scaling Relationships in Standardized Rainfall Fluctuations and Their Use in Spatial Disaggregation Schemes

Let $\overline{I_L}$ denote the value of the average rainfall intensity at a particular pixel of size L, and let $I'_{L,i}$ denote the value of the rainfall fluctuation (difference between the value at the adjacent pixel and the value at the particular pixel of interest) at the same scale L and direction i (e.g., i=1, 2, 3 for latitudinal, longitudinal, and diagonal directions, respectively). Standardized rainfall fluctuations at scale L and direction i are defined as $\xi_{i,L} = I'_{L,i}/\overline{I}_L$. *Perica and Foufoula-Georgiou* [1996a] computed multiscale standardized rainfall fluctuations using an orthogonal Haar wavelet decomposition and found that at least between the scales of 4 and 64 km for which data were available, $\xi_{i,L}$ exhibited normality and simple scaling, implying that

$$\frac{\sigma_{\xi,L_1}}{\sigma_{\xi,L_2}} = \left(\frac{L_1}{L_2}\right)^H \tag{1}$$

where $\sigma_{\xi,L}$ is the standard deviation of ξ at scale L km and H is a scale-independent parameter. The values of H varied between 0.2 and 0.5 for several midlatitude mesoscale convective systems from the PRE-STORM (Preliminary REgional Experiment for STORM-Central) data set [e.g., *Cunning*, 1986]. The dependence of H on direction was not very pronounced, but H was found to be strongly dependent on the convective instability of the prestorm environment, as measured by the convective available potential energy (CAPE) (in $m^2\ s^{-2}$):

$$H = 0.0516 + 0.9646(\text{CAPE} \times 10^{-4}) \tag{2}$$

This is a very useful relationship since CAPE can be computed from observed sounding data or by a numerical weather prediction model (see also *Zhang and Foufoula-Georgiou* [1997] for the selection of a representative value of CAPE) and then H can be estimated from (2) and used via (1) to infer the variability of rainfall fluctuations at any scale given the variability at a reference scale. Then, based on an inverse filtering pro-

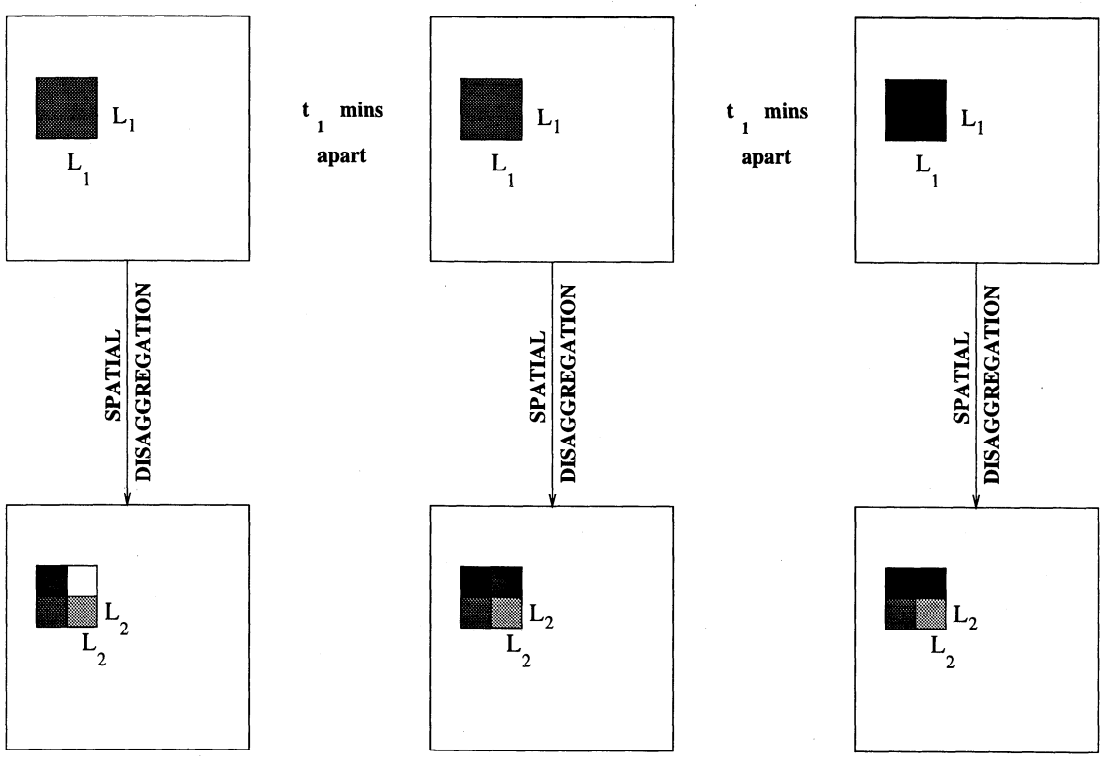

Figure 1. Implementation of a spatial disaggregation scheme independently at various instants in time.

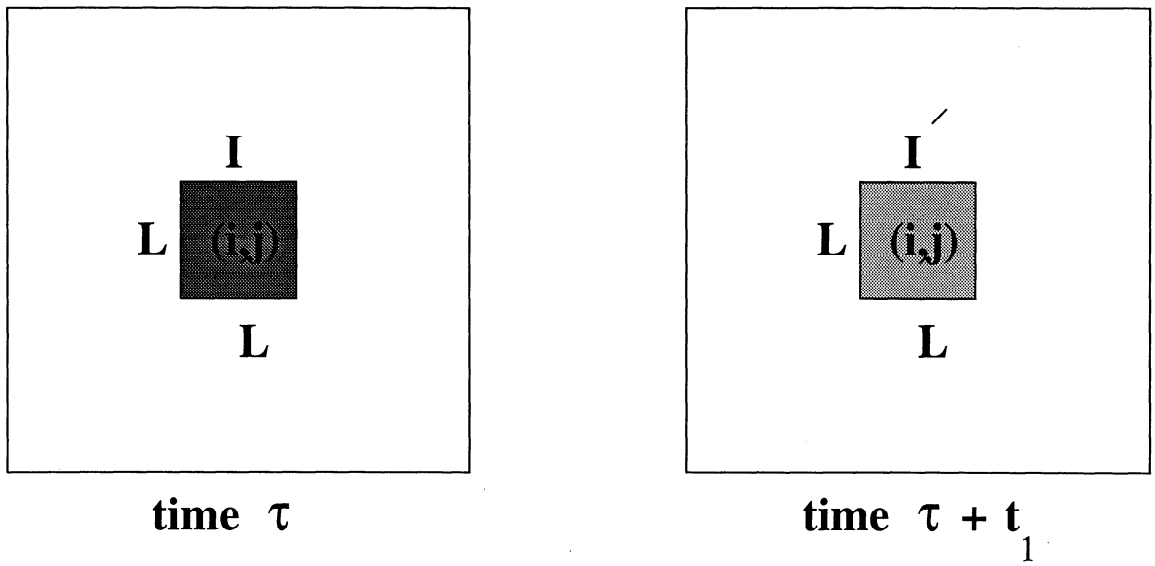

Figure 2. Schematic illustrating the change in intensity of a field (rainfall in this case) over a box of size $L \times L$ (scale L) centered around the location (i, j) during a time interval t.

cedure, these fluctuations at different scales, together with the initial large-scale average field, can be used to statistically reconstruct the subgrid-scale spatial variability of rainfall (for details, see *Perica and Foufoula-Georgiou* [1996b]).

To downscale evolving rainfall fields, one could implement the above spatial disaggregation scheme independently at each instant of time (see schematic in Figure 1) using appropriate values of the evolving parameter, CAPE. The drawback with such an approach is that the temporal persistence (correlation) that exists in reality at the subgrid spatial scales is not reproduced by the model. This is a problem since temporal persistence in rainfall directly relates to the spatial variability of accumulated local soil moisture and might be important if the downscaled values were to be used in a coupled atmospheric-hydrologic model. To incorporate temporal persistence at these small scales, we studied how the evolution of rainfall at large space-time scales relates to the evolution at smaller scales. The results were extensively presented by *Venugopal et al.* [1999] and are briefly summarized in the next section.

2.2. Summary of Space-Time Scale Invariance in Rainfall Evolution

Let $I_{L,\tau}(i,j)$ and $I_{L,\tau+t}(i,j)$ represent rainfall intensity values averaged over a box of size L (typically in kilometers) centered around spatial location (i,j), at two instants of time, τ and $\tau + t$ (I and $I^{'}$ in Figure 2). The evolution of the entire field over a time period t and over spatial scale L could be measured by a statistical description of the intensity differences, i.e., $[I_{L,\tau+t}(i,j) - I_{L,\tau}(i,j)]$, taken at all spatial locations (i,j). Such a statistical description would be appropriate only for a process which is additive, i.e., for a process for which increments are independent of the background intensity ($(I^{'} - I) = \epsilon$, where ϵ is an independent identically distributed random variable). However, for a multiplicative process for which increments are dependent on the background intensity, and specifically for a process for which $I^{'}/I = \epsilon$ or $I^{'} - I/I = \epsilon^{'}$, it would be more appropriate to study the standardized increments ($(I^{'} - I)/I \equiv \Delta I/I$) of the process or the differences in the log of the process, since log(process) is additive ($lnI^{'} - lnI \equiv \Delta lnI = \epsilon^{''}$). Thus, on the basis of evidence that relative changes in spatial fluctuations are independent of intensities [*Perica and Foufoula-Georgiou*, 1996a] and that relative changes in temporal fluctuations are also independent of the intensities [e.g., see *Venugopal et al.*, 1999, Figure 2], we choose to measure rainfall evolution at spatial scale L and time lag t by a statistical characterization of the field:

$$\Delta lnI(L,t) \equiv lnI_L(\tau + t) - lnI_L(\tau) \qquad (3)$$

where $I_L(\tau)$ denotes the rainfall intensity at spatial scale L and time instant τ and t represents the time lag over which the rainfall evolution is measured.

As was extensively discussed by *Venugopal et al.* [1999], the dependence of $\Delta lnI(L,t)$ on location (i,j) is eliminated assuming that the field $\Delta lnI(L,t)$ is statistically homogeneous in space, and thus a single probability density function (PDF) over all locations can be formed. Also, the dependence of $\Delta lnI(L,t)$ on the exact time τ is eliminated by working within regions in time where its statistical properties do not vary significantly around their mean values over the region.

On the basis of analysis of various storms from Darwin, Australia, it was found that the $\Delta lnI(L,t)$ fields were spatially uncorrelated [e.g., see *Venugopal et al.*, 1999, Figure 3] and that the PDF of $\Delta lnI(L,t)$ exhibited Gaussian behavior, at least for time intervals of

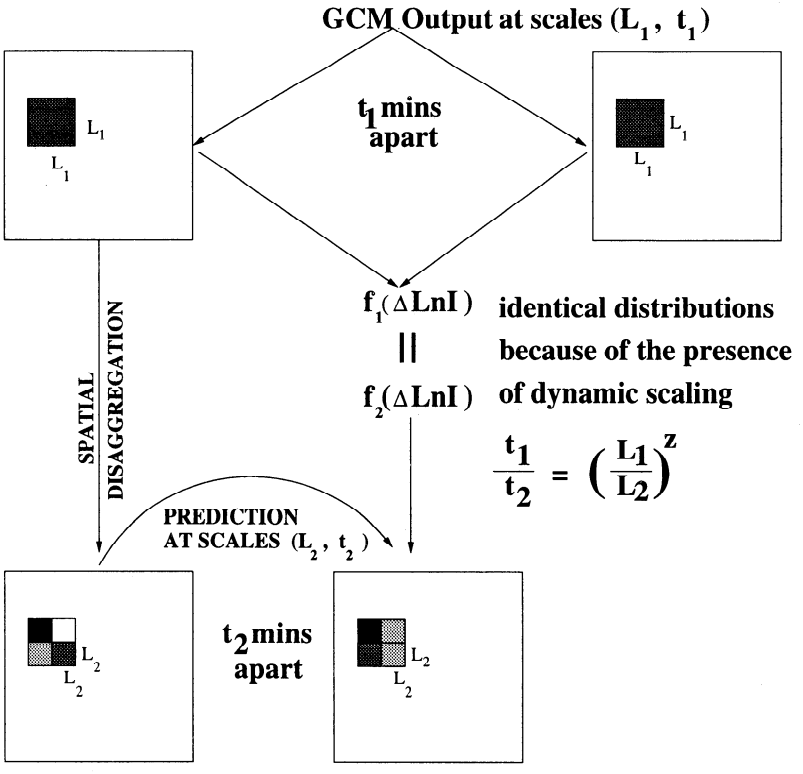

Figure 3. Schematic of space-time downscaling illustrating how the framework of dynamic scaling is coupled with a spatial disaggregation scheme to predict rainfall evolution at smaller space-time scales. In brief, the PDF (probability density function) $f_1(\Delta lnI)$ is first evaluated from the known large-scale fields, i.e., the fields at spatial scale L_1 and temporal scale t_1. Then, given the spatial scale L_2 down to which we want to disaggregate, the corresponding time lag t_2 is computed from the power-law relationship (equation (4)). Dynamic scaling implies that the PDF, $f_2(\Delta lnI)$, at scales (L_2, t_2) is identical to that at scales (L_1, t_1), i.e., $f_1(\Delta lnI) = f_2(\Delta lnI)$. Then, $f_2(\Delta lnI)$ is used to statistically predict the evolution of the rainfall field at small space-time scales.

10-80 min and spatial scales of 2-32 km, for which data were available. In addition, it was also found that under transformations of the type $t \sim L^z$ (where z is called the dynamic scaling exponent), the rainfall field evolution characterized by the PDF of $\Delta lnI(L,t)$ remained statistically invariant (for details, see *Venugopal et al.* [1999]).

To understand the significance of such a statistical scale-invariance, let us, for example, consider $z = 0.8$, an average value of z found from rainy season rainfall fields in Darwin, Australia. The presence of dynamic scaling tells us that the PDFs of ΔlnI remain the same as long as

$$\frac{t_1}{t_2} = \left(\frac{L_1}{L_2}\right)^z \tag{4}$$

For example, consider two features of sizes 16 km (L_1) and 2 km (L_2). From (4) it is clear that the time it takes for the smaller feature to undergo the same evolution that the larger feature would undergo in time t_1 is

$$t_2 = t_1 \left(\frac{2}{16}\right)^{0.8} \approx 0.2t_1 = t_1/5;$$

that is, the rate of change of the 8-times-smaller feature is 5 times faster. Note that the rate of evolution does not depend on the actual sizes of the two features, but only on their ratio.

3. Space-Time Downscaling Model

3.1. Basic Scheme

Given the output of a mesoscale numerical weather prediction model, i.e., average precipitation intensities on, for instance, grid boxes of size 32 km, one could use the above developments for space-time rainfall downscaling. (Note that we work with dyadic scales for convenience of algorithm implementation.) The proposed downscaling model is depicted in Figure 3. The idea behind the model comes from evidence that the rate of evolution at larger space-time scales is related to the

rate of evolution at smaller scales (dynamic scaling). If this is incorporated into the space-time downscaling model, temporal persistence in the small-scale spatial fields is statistically ensured.

First, the space-time downscaling model utilizes a spatial disaggregation scheme to downscale from the typical spatial scale of a global or regional climate model output (say, L_1) at one instant of time to a finer spatial scale of hydrologic interest (say, L_2); for instance, from 32 km down to 2 km. Here the spatial downscaling scheme of *Perica and Foufoula-Georgiou* [1996b] was used, but any other spatial disaggregation scheme could have been employed as well. Second, using the global or regional climate model output at the spatial scale L_1, and at two instants of time t_1 min apart, the PDF of $\Delta lnI(L_1, t_1)$ is evaluated. The evidence of dynamic scaling suggests that the PDF of $\Delta lnI(L_1, t_1)$ (denoted by f_1 in Figure 3) is identical to the PDF of $\Delta lnI(L_2, t_2)$ (f_2 in Figure 3), i.e., the PDF at the desired small-scale L_2, if and only if the associated time lag t_2 is given by

$$t_2 = t_1 \left(\frac{L_2}{L_1}\right)^z$$

By knowing f_2 and the fine-scale output from the spatial disaggregation model at the "initial" time instant τ, one could then predict the rainfall field at the time instant $\tau + t_2$ min later and at the same fine spatial scale, L_2. Assuming that the field ΔlnI at the small-scale (L_2, t_2) remains statistically stationary in time within at least a time period equal to the larger-scale time lag t_1, f_2 can be used to predict the small-scale field at time instants $\tau + t_2$, $\tau + 2t_2$, etc., up to $\tau + t_1$. (The period t_1 of stationarity in ΔlnI was taken to be 10 min in our downscaling application.)

The prediction of the rainfall field at the small-scale L_2 and at time $\tau + t_2$, given the field at time τ and the PDF of $\Delta lnI(L_1, t_1) = f_1$, is based on the dynamic scaling assumption, which implies that if (4) holds,

$$\{lnI_{L_2}(\tau + t_2) - lnI_{L_2}(\tau)\} \stackrel{d}{=} \{lnI_{L_1}(\tau + t_1) - lnI_{L_1}(\tau)\} \tag{5}$$

where $\stackrel{d}{=}$ stands for equality in distribution. Denoting by r the random variable in the right-hand side of (5), i.e., $r \equiv lnI_{L_1}(\tau + t_1) - lnI_{L_1}(\tau)$ (which we know from the known PDF, f_1, at the large scale), and solving for $lnI_{L_2}(\tau + t_2)$, we get

$$lnI_{L_2}(\tau + t_2) = lnI_{L_2}(\tau) + r \tag{6}$$

$$\Longrightarrow I_{L_2}(\tau + t_2) = I_{L_2}(\tau) * e^r \tag{7}$$

Note that the assumption of a multiplicative nature of rainfall as discussed earlier implies that r is independent of I. Thus one could generate r from the PDF of $\Delta lnI(L_1, t_1)$ and proceed with the statistical prediction of rainfall following (7). Notice from (6), however, that

$$\mathrm{var}(lnI_{L_2}(\tau + t_2)) = \mathrm{var}(lnI_{L_2}(\tau)) + \mathrm{var}(r)$$

from which it is clear that the variance of the log of the predicted field $I_{L_2}(\tau + t_2)$ increases linearly with time. Consequently, the predicted field becomes progressively rougher and the spatial correlation of the field decreases correspondingly. (As expected, this was noticed as speckling in the predicted rainfall fields.) Thus a "smoothing" procedure needs to be introduced, the objective of which would be to prevent $\sigma(lnI)$ of the predicted fields from increasing indefinitely in time.

Heuristically, a smoothing can be achieved by ensuring that points of the lnI field (in space) with negative curvature (local maxima) are more likely to decrease and those with positive curvature (local minima) are more likely to increase, i.e., introduce changes ($\Delta lnI = r$) which depend on the curvature of lnI, but are still independent of the intensity of I. By balancing roughening and smoothing, one can either preserve $\sigma(lnI)$ in time (i.e., temporal stationarity of log(rainfall)) or change $\sigma(lnI)$ in a controlled fashion depending on the constraints of the problem. We discuss how this can be implemented in the case of space-time downscaling of rainfall in the next section.

3.2. Preservation of $\sigma(lnI)$ During Evolution

The issue of finding a balance between roughening and smoothing, so that $\sigma(lnI)$ does not increase indefinitely with time, is addressed by introducing a tuning factor in the form of probability, i.e., assign changes based on (some) probability p. In other words, if C_{lnI} denotes the curvature (in space) of lnI, we implement the following scheme: If $C_{lnI} > 0$, then $r = |r|$ with probability p and $r = r$ with probability $1 - p$. If $C_{lnI} < 0$, then $r = -|r|$ with probability p and $r = r$ with probability $1 - p$. Thus positive curvature points are incremented (positive change) with probability p, and negative curvature points are decremented (negative change) with the same probability. While $p = 0$ (no smoothing at all) corresponds to rougher and rougher predicted fields (increasing standard deviation going up to ∞ and decreasing spatial correlation), $0 < p < 1$ corresponds to smoother (relative to $p = 0$) predicted fields (finite standard deviation). When $p = 1$, the smoothest predicted fields (minimum standard deviation) possible in the framework of this procedure are attained.

Assigning the same probability p to positive and negative changes would not change the distribution of ΔlnI, if the number of positive curvatures (denoted by $n_{C>0}$) is approximately the same as the number of negative curvatures (denoted by $n_{C<0}$). If this is not the case (as was found for rainfall), the distribution of changes ($r = \Delta lnI(t_1, L_1)$) which was found to be Gaussian with zero mean and some standard deviation [see *Venugopal et al.*, 1999], will change. In other words, the distribution of r would, in time, have a positive or negative mean (instead of zero) depending on higher number of positive or negative curvatures, respectively.

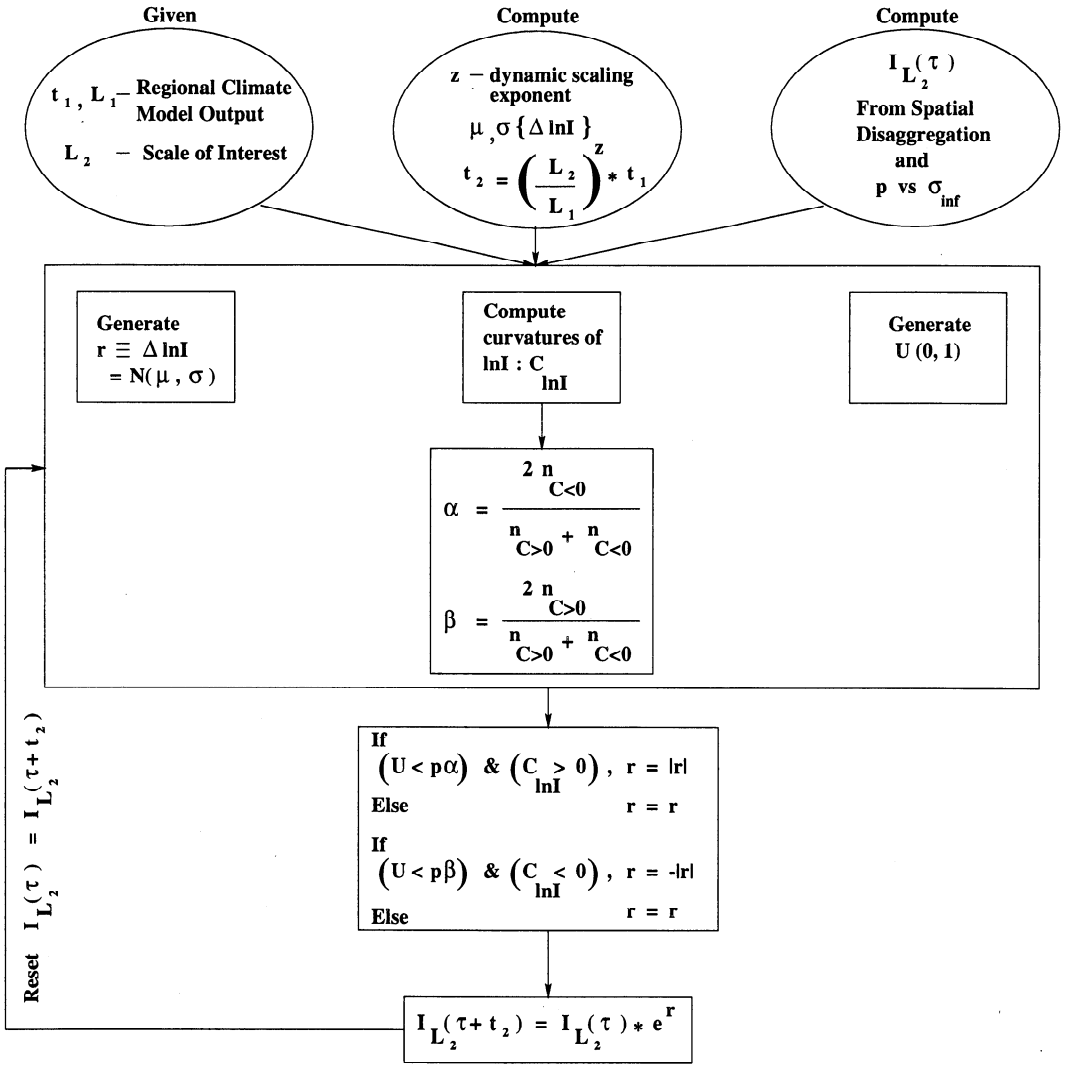

Figure 4. Flowchart of the proposed space-time downscaling model (see text for terminology).

This would, in turn, introduce a bias in the predicted fields. For instance, if $n_{C<0} > n_{C>0}$, "mass" is consistently removed at a higher rate than it is added, with the result that the mean and standard deviation of the log(rainfall) decrease with time.

To preserve the distribution of ΔlnI in accordance with the assumption of temporal stationarity of ΔlnI within at least a time period equal to t_1, we define two "correction" factors α and β:

$$\alpha = \frac{2n_{C<0}}{(n_{C<0}+n_{C>0})}$$
$$\beta = 2 - \alpha;$$

i.e., α and β represent the proportion of the number of negative and positive curvatures, respectively. The purpose of introducing these factors is to even out the number of negative and positive changes and not allow any systematic bias in the predicted fields. Notice that the role of p as a tuning factor still remains; that is, it is introduced to ensure that $\sigma(lnI)$ does not increase indefinitely (the case corresponding to $p = 0$) with time and the processes of roughening and smoothing appropriately balance each other. Thus, in the new scheme, changes ($r = \Delta lnI$) are now assigned with probabilities which are a function of the proportion of the number of positive or negative curvatures; that is, if $C_{lnI} > 0$, then $r = |r|$ with probability $p\alpha$ and $r = r$ with probability $p(1 - \alpha)$. If $C_{lnI} < 0$, then $r = -|r|$ with probability $p\beta$ and $r = r$ with probability $p(1 - \beta)$.

As a simple example, consider $n_{C<0} > n_{C>0}$. From the definition of α and β, it is clear that $\alpha > \beta$. However, the correction factors in the scheme ensure that the number of positive and negative changes are the same, since points of positive curvature have a higher probability of being assigned a positive change as compared with points of negative curvature being assigned a negative change. This, in turn, ensures that the initial distribution of r is not distorted. The flowchart in Figure 4 shows the proposed downscaling model in its entirety.

3.3. Determination of the Factor p

The role of the tuning factor p, which achieves a balance between roughening and smoothing, is qualitatively known; that is, $p = 0$ leads to infinite $\sigma(lnI)$, while $0 < p < 1$ results in finite $\sigma(lnI)$ with time. It remains to study the effect of p on the statistics of the predicted fields in a quantitative sense. The illustrative example presented here is for the storm of January 4, 1994, over Darwin, Australia (see *Venugopal et al.* [1999] for a description of this storm). For this storm, the large-scale fields ($L_1 = 32$ km) were available every $t_1 = 10$ min. The small-scale field ($L_2 = 2$ km) at the initial time instant was obtained from the large-scale field using the spatial disaggregation scheme of *Perica and Foufoula-Georgiou* [1996b] (see the next section for more details).

Then, the previously described algorithm based on dynamic scaling was applied to predict rainfall fields every 1 min up to 100 min. (The value of z used was equal to 0.8, and the prediction was done every 1 min since (4) implies that $t_2 = 10 \times (2/32)^{0.8} \approx 1$ min; see the next section for more details on the implementation.) This experiment was repeated for different values of p ($p = 0, 0.1, \cdots, 1$) kept constant over the prediction period of 100 min. Figure 5 shows the variation of the standard deviation of the predicted (lnI) fields with time at the spatial scale of 2 km. As can be seen from this figure, for $p = 0$, $\sigma(lnI)$ increases indefinitely with time; for $0 < p < 1$, $\sigma(lnI)$ reaches a finite asymptotic value which depends on the value of p, and for $p = 1$, the least $\sigma(lnI)$ is obtained. Thus any $0 < p < 1$ results, asymptotically in time, in a field with finite $\sigma(lnI)$ (denoted by σ_∞).

The dependence of σ_∞ on p is shown in Figure 6. It is worth mentioning here that this σ_∞-versus-p curve is dependent on the connectivity of the initial rainfall field, i.e., the statistical structure of the rain-covered areas. This is because given enough time to evolve, for the same value of p, fields which initially had larger rain-covered areas will develop larger wavelength features (up to the size of the largest rain-covered area) and of larger amplitude and thus would attain a larger asymptotic value of σ_∞. Thus, in the implementation stage, once the initial fine-scale rainfall field is given, the corresponding σ_∞-versus-p curve must be constructed on-line to be used in the space-time downscaling.

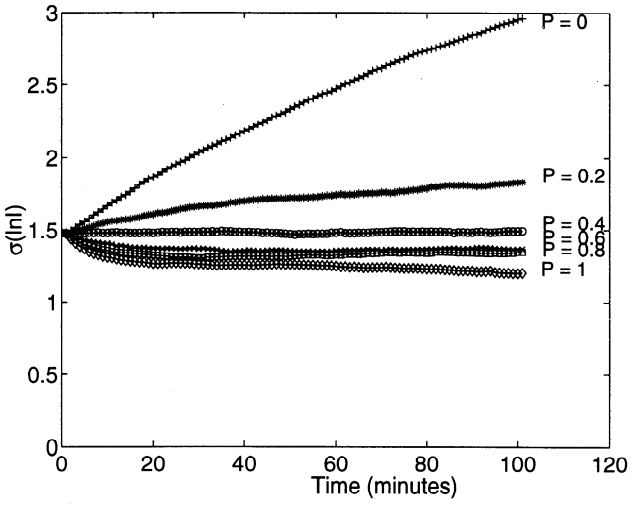

Figure 5. Storm of January 4, 1994, over Darwin, Australia: temporal variation of σ_{lnI} of the predicted fields using the proposed space-time downscaling model, for different values of p.

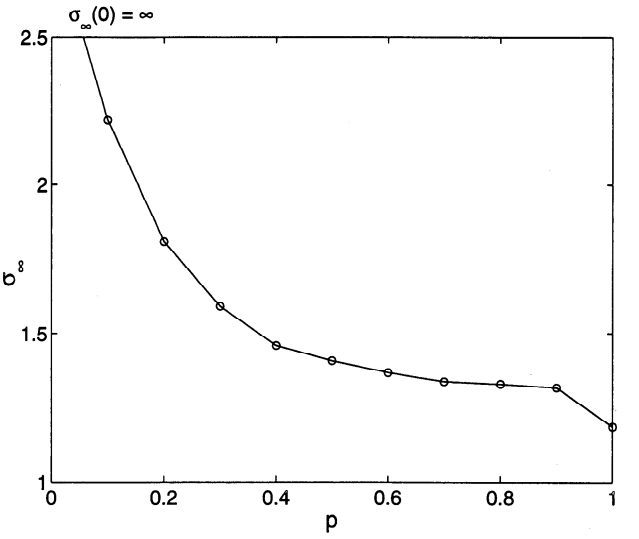

Figure 6. Storm of January 4, 1994, over Darwin, Australia: variation of σ_∞ with p.

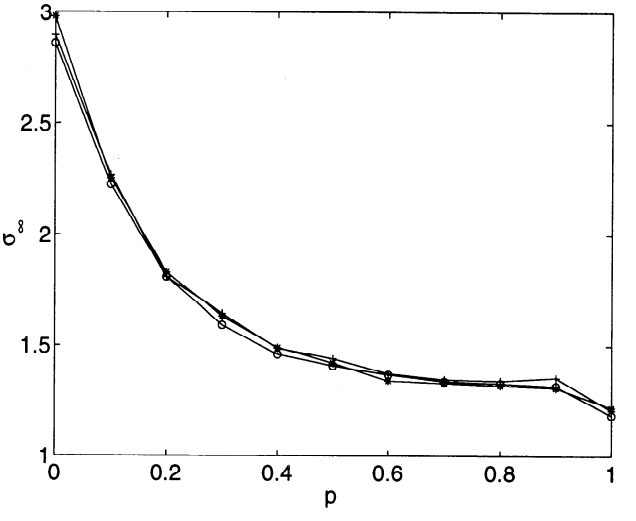

Figure 7. Storm of January 4, 1994, over Darwin, Australia: variation of σ_∞ with p for different realizations from the spatial disaggregation scheme of *Perica and Foufoula-Georgiou* [1996b]. The closeness of the curves shows that the spatial disaggregation scheme does not change the connectivity structure of the initial subgrid-scale field enough to significantly alter the σ_∞-versus-p relationship.

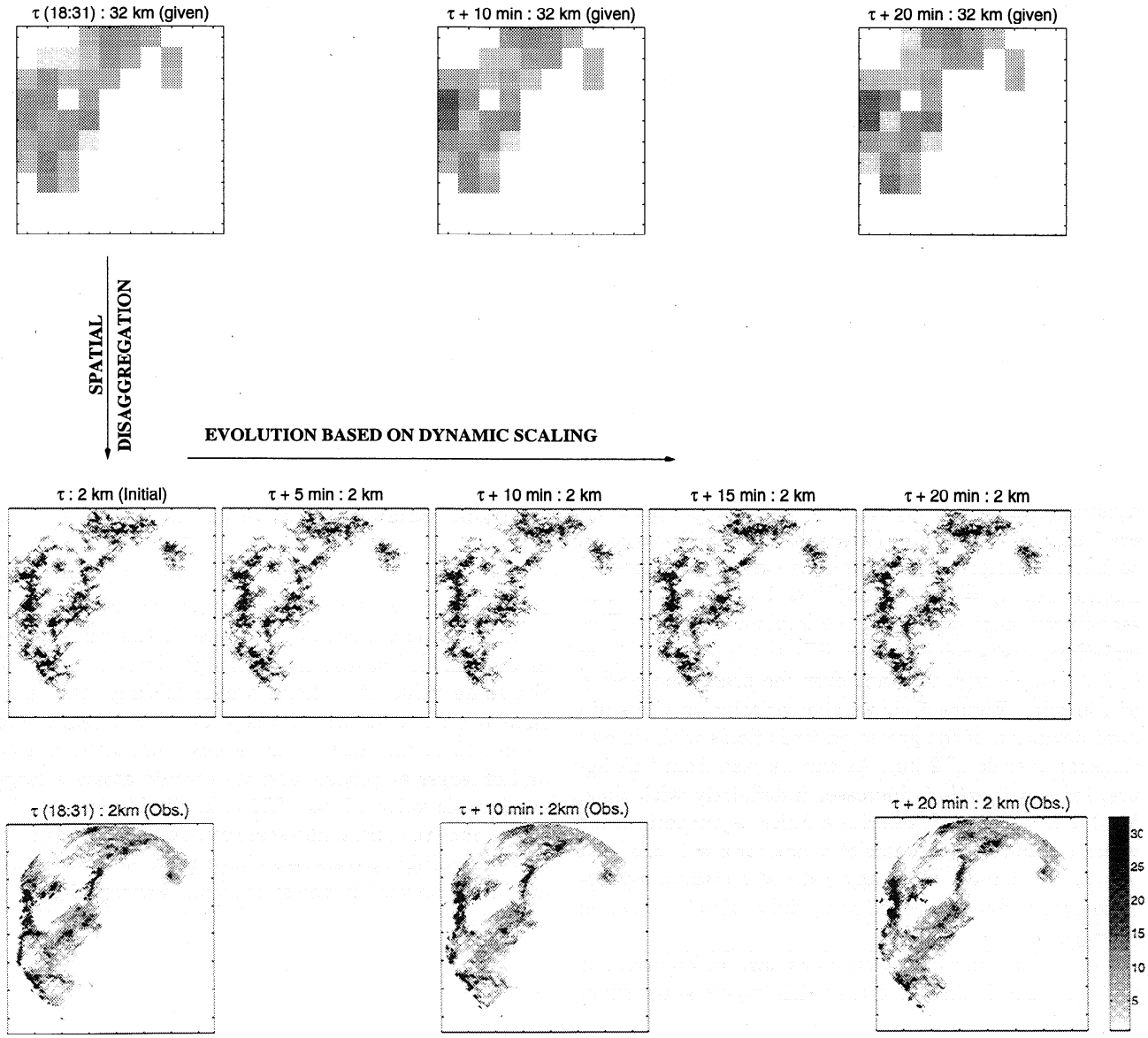

Figure 8. Implementation of the model shown in Figure 4 on the storm of January 4, 1994, in Darwin, Australia. The top row shows the given large-scale fields (here at the scale of 32 km and every 10 min). The leftmost panel in the middle row shows the spatially disaggregated field at the scale of 2 km and the remaining panels in the same row show the predicted fields at times $\tau = 5$, 10, 15 and 20 min, using the developed space-time downscaling model. The bottom row shows the observed fields at the scale of 2 km and every 10 min for comparison.

Recall that the initial subgrid-scale field (with its given connectivity structure) comes from a statistically based spatial disaggregation scheme. To check the sensitivity of the σ_∞-versus-p curve to the statistical variability of the initial connectivity structure, multiple realizations of spatially downscaled fields were obtained from the scheme of *Perica and Foufoula-Georgiou* [1996b] and the σ_∞-versus-p dependence was evaluated for each of these realizations. Figure 7 shows that the σ_∞-versus-p curve does not significantly change from one realization to another. This gives us the confidence to adopt this curve in our downscaling model as the basis for finding the value of p that would evolve an initial field with a particular initial connectivity to a field having a desired $\sigma(lnI)$ ($\equiv \sigma_\infty$), provided that the allowed evolution time is enough to reach this asymptotic value of σ.

4. Implementation

The proposed space-time downscaling model was implemented on several rainy season convective storms in Darwin, Australia, for which dynamic scaling was documented by *Venugopal et al.* [1999]. Here the results of the implementation are presented only for one event, the storm of January 4, 1994. Similar results were

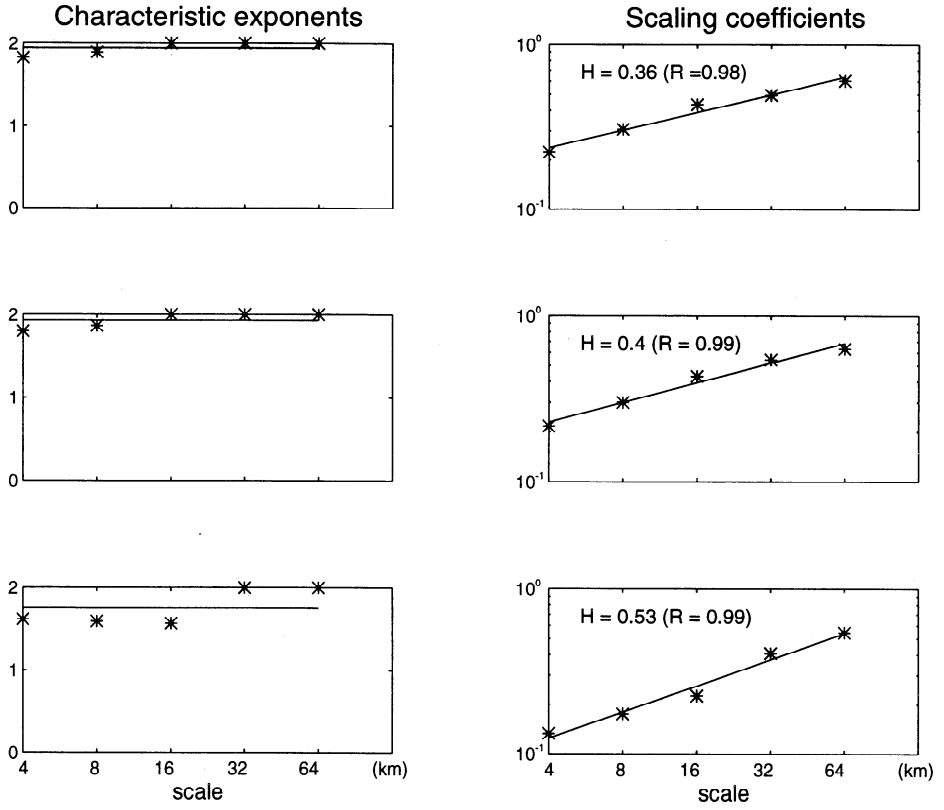

Figure 9. Storm of January 4, 1994 over Darwin, Australia. For the frame at time 2331 UTC, the plots in the left column show that the standardized spatial fluctuations are well approximated by a Gaussian distribution (i.e., stable distribution with parameter = 2). The plots in the right column show that the standardized spatial rainfall fluctuations exhibit simple scaling (log-log linearity of standard deviation with scale), with H equal to 0.36, 0.4, and 0.53 for the latitudinal, longitudinal, and diagonal components, respectively. A value of $H = 0.4$ was adopted for this frame to use in its spatial downscaling. Similar results were obtained for the other frames of this storm.

found for other storms and are documented by *Venugopal* [1999].

The storm of January 4, 1994 was analyzed by *Venugopal et al.* [1999], and it was found that it obeys dynamic scaling within several periods over which the ΔlnI field remains stationary. Rainfall fields at a scale of 2 km were available to us every 10 min. Upscaling (by simple spatial averaging) was performed on these fields to construct large-scale fields at $L_1 = 32$ km every $t_1 = 10$ min. These fields (top row in Figure 8) were the starting point of our implementation; that is, they were interpreted as the outputs of a mesoscale or global circulation model which needed to be downscaled for hydrologic applications. The desired scale of downscaling was taken to be $L_2 = 2$ km.

The part of the storm for which we present our results starts at $\tau = 2331$ UTC. For this part of the storm, *Venugopal et al.* [1999] found that the dynamic scaling exponent z had a value of $\sim$0.8, and this is the value of z that we adopted here for the space-time downscaling model. Given this information and based on the dynamic scaling relation, we get $t_2 = t_1 \times (L_2/L_1)^z = 10 \times (2/32)^{0.8} \approx 1$ min. Thus the proposed downscaling model, in conjunction with the spatial disaggregation scheme of *Perica and Foufoula-Georgiou* [1996b] can predict the rainfall field evolution every 1 min at the subgrid scale of 2 km.

First, to verify that the spatial downscaling scheme of *Perica and Foufoula-Georgiou* [1996b] is appropriate for this storm, the standardized spatial fluctuations (see section 2) at several time instants were analyzed for the presence of normality and simple scaling. For example, for the initial time instant at which we start the downscaling model ($\tau = 2331$ UTC), Figure 9 demonstrates the presence of normality in the standardized rainfall fluctuations (the stable distribution parameter $\sim$2) and simple scaling in the standard deviation of all three directional components of the standardized fluctuations (log-log linearity of the standard deviation with scale). The scaling parameter H varies slightly for each directional component between 0.38 and 0.5. Similar results were obtained for the spatial rainfall fields at other time instants. Here we have adopted a value of $H = 0.4$ for the spatial downscaling. Using this value of H and the spatial disaggregation scheme of *Perica and Foufoula-Georgiou* [1996b], we obtained a rainfall field at the scale of 2 km and time instant $\tau = 2331$ UTC. This is the leftmost panel in the middle row of Figure 8.

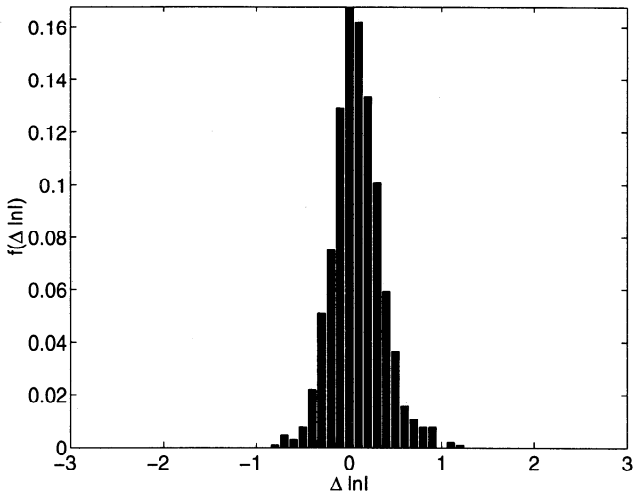

Figure 10. Storm of January 4, 1994, in Darwin, Australia: the PDF of ΔlnI at a spatial scale of 32 km and time lag of 10 min.

For this initial 2 km rainfall field, the σ_∞-versus-p curve was computed as discussed in the previous section, and it was stored to be used in the evolution of the fine-scale field. Next, the PDF of $\Delta lnI(L_1 = 32$ km, $t_1 = 10$ min) was computed from the large-scale fields at times τ and $\tau + 10$ min. According to the dynamic scaling hypothesis with $z \approx 0.8$, this PDF (shown in Figure 10) is considered to be identical to the PDF of $\Delta lnI(L_2 = 2$ km, $t_2 = 1$ min) and can be used to generate r needed in (7). It should be noted that the dynamic scaling hypothesis was verified by *Venugopal et al.* [1999] via extensive analysis for temporal scales of $t = 10, 20, \cdots, 80$ min and spatial scales of $L = 2, \cdots, 16$ km for which data were available.

In this paper, an extrapolation is made that this hypothesis holds down to temporal scales of 1 min and extends up to spatial scales of 32 km. For the latter, we have enough evidence to believe that this is a valid extrapolation since for all cases for which enough data at the 32-km scale were available, dynamic scaling was extending to this spatial scale, too. For the extrapolation down to 1 min, no direct verification can be done since no spatial data are available every 1 min. The validity of this hypothesis can only be tested indirectly by comparing the predicted fields with the observed ones every 10 min, as is done in section 5 of this paper. If the prediction performs well and given that there is no theoretical reason to believe that there would be a breakdown of dynamic scaling below 10 min, the hypothesis of extrapolating the presence of dynamic scaling to a temporal scale of less than 10 min is not rejected.

It is noted that although the predictive model could be applied indefinitely in time to predict small-scale rainfall fields given an initial small-scale field, we preferred to update the prediction by recomputing the PDF of $\Delta lnI(L_1, t_1)$ every time a new large-scale field became available, i.e., every 10 min in our case. Also, the spatial disaggregation scheme of *Perica and Foufoula-Georgiou* [1996b] was applied at all times that a new large-scale precipitation field became available (i.e., every $t_1 = 10$ min), and although the exact rainfall intensities of the spatially downscaled fields were not directly used in the evolution, $\sigma(lnI)$ at the small scale L_2 (2 km) was computed for each of these subgrid-scale fields. This was done in order to get an approximation (by linear interpolation) of the temporal variation of $\sigma(lnI)$ at $L_2 = 2$ km every 1 min, given its values every 10 min. These interpolated values were then used to obtain the value of p from the σ_∞-versus-p curve.

In other words, we always evolved the initial field at some time instant τ to a new field t_2 min later such that $\sigma(lnI)$ ($\equiv \sigma_\infty$) of the evolved field is equal to the interpolated value $\sigma(lnI)(\tau + t_2)$. In using this procedure, we made an assumption that the time period t_2 min is enough to go from a field with standard de-

Table 1. For the January 4, 1994, Australia, Storm, a Comparison of the Unconditional and Conditional ($I > 0$) Mean and Standard Deviation of the Predicted and Observed Instantaneous Rainfall Intensity Fields at $\tau = 0$, 10, 20, 30, 40 and 50 min and at a Spatial Scale of 2 km

Statistics *	Initial Field	10 Min	20 Min	30 Min	40 Min	50 Min
$\mu(I)$						
Predicted	0.82	0.78	0.77	0.72	0.67	0.66
Observed	0.82	0.80	0.78	0.74	0.68	0.63
$\sigma(I)$						
Predicted	3.75	3.57	3.58	3.20	2.75	2.63
Observed	3.57	3.43	3.12	2.98	2.75	2.52
$\mu(I/I > 0)$						
Predicted	5.80	5.48	5.43	5.11	4.77	4.69
Observed	6.08	5.83	5.74	5.61	5.22	4.85
$\sigma(I/I > 0)$						
Predicted	8.41	8.02	8.08	7.08	5.81	5.47
Observed	7.93	7.51	6.55	6.31	5.86	5.36

*Values are given in mm h^{-1}.

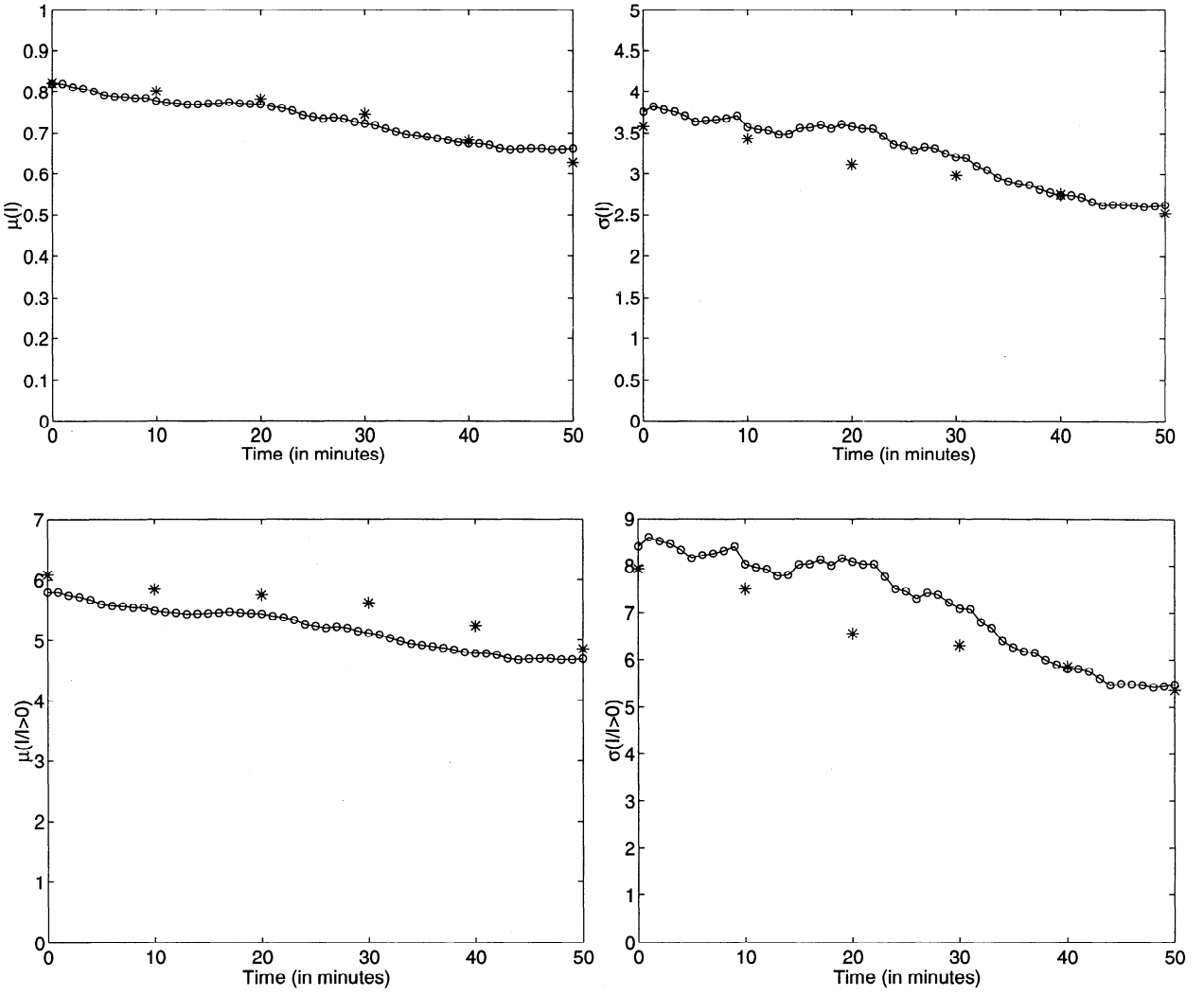

Figure 11. Storm of January 4, 1994, over Darwin, Australia: comparison of the unconditional (top row) and conditional (bottom row) mean and standard deviation, of the predicted fields (circles) and the observed fields (asterisks) at a spatial scale of 2 km.

viation $\sigma(lnI)(\tau)$ at time instant τ to a field with an asymptotic standard deviation of $\sigma_\infty = \sigma(lnI)(\tau + t_2)$ at time instant $\tau + t_2$. This is a valid assumption since $\sigma(lnI)$ does not change significantly in that short period of time, i.e., $t_2 = 1$ min. Progressing in this fashion, i.e., choosing a new value of p every t_2 min (depending on the interpolated value of $\sigma(lnI)(\tau+t_2)$), at the end of t_1 min we reach the desired value of $\sigma(lnI)(\tau + t_1)$ which was already computed from the spatially disaggregated field.

Figure 8 shows the given fields at the scale of 32 km and every 10 min (top row), the disaggregated field at the scale of 2 km and $\tau = 0$ obtained by the spatial disaggregation scheme of *Perica and Foufoula-Georgiou* [1996b] (leftmost panel in the middle row), and the predicted fields at time instants 5, 10, 15, and 20 min later, using the proposed downscaling model. The bottom row of Figure 8 shows the observed fields at the scale of 2 km every 10 min. It is noted that visually, the predicted fields resemble the observed fine-scale fields. A detailed quantification of the model performance is given in the next section.

5. Model Performance

Several measures have been used to quantitatively evaluate the performance of the proposed space-time downscaling model. Generally, we want to check how the mean, standard deviation, percentage of rain-covered area, and spatial and temporal correlations of rainfall intensities at the subgrid scales have been preserved.

For the storm of January 4, 1994, in Darwin, Australia, Table 1 shows the mean and standard deviation of the instantaneous rainfall intensities over the domain of the radar (an area of 300 × 300 km), i.e., $\mu(I)$ and $\sigma(I)$, and over the rain-covered area only, i.e., the conditional mean and standard deviation, $\mu(I/I > 0)$ and $\sigma(I/I > 0)$, of the predicted and observed fields at a

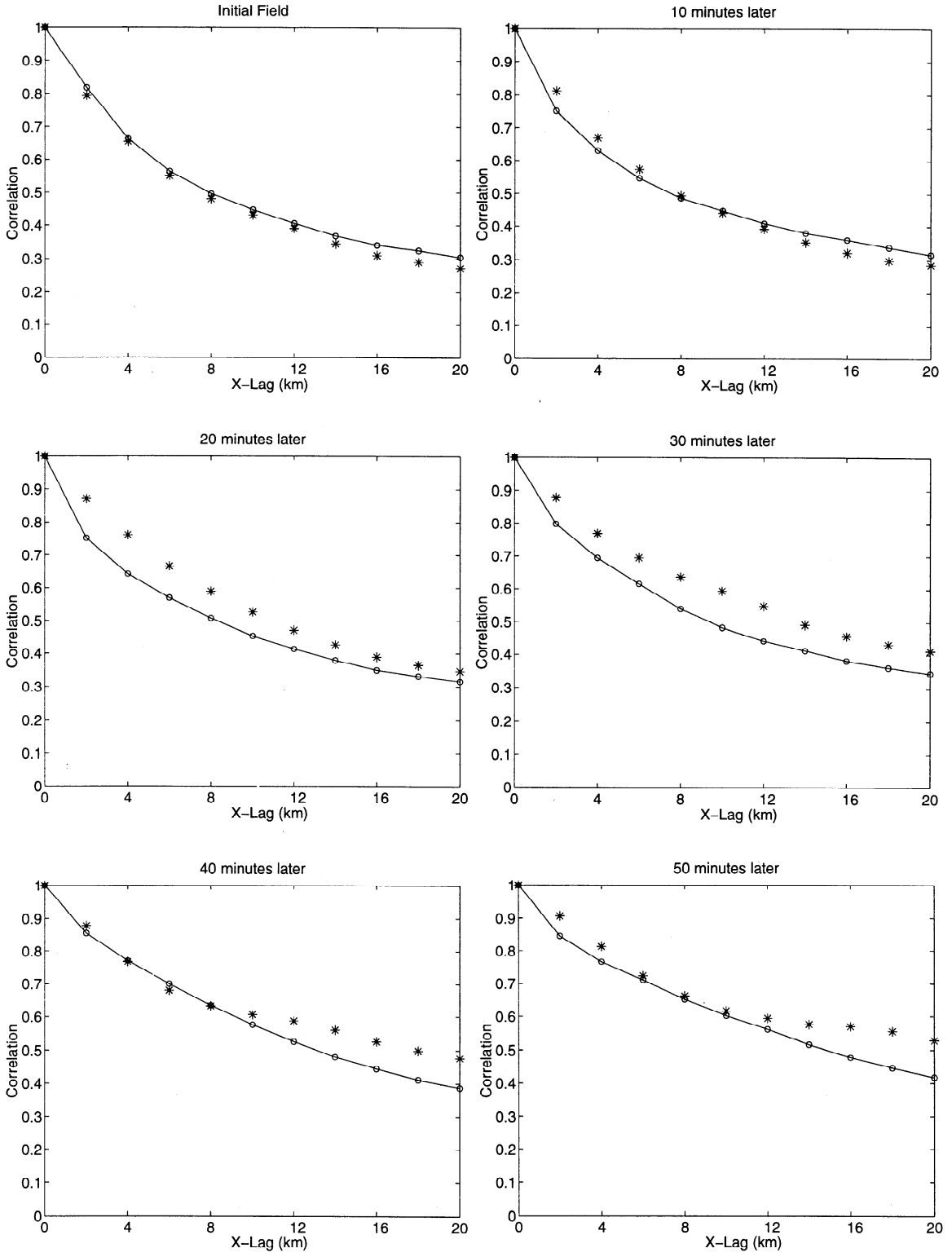

Figure 12. Storm of January 4, 1994: comparison of the spatial correlation in the X direction of the observed fields (asterisks) and the predicted fields (circles) at a spatial scale of 2 km and at time instants $\tau = 0, 10 \cdots, 50$ min. Similar plots were found for the Y direction, as the field is almost isotropic.

spatial scale of 2 km and at times $\tau = 0, 10, 20, \cdots, 50$ min. A good agreement is observed in the unconditional statistics, and no trend of consistent overestimation or underestimation is observed. Given that the spatial disaggregation scheme underestimated the conditional mean of the initial field at $\tau = 0$ and overestimated the conditional standard deviation (note that the spatial disaggregation scheme exactly preserves only the unconditional mean), the conditional mean is slightly underestimated and the conditional standard deviation

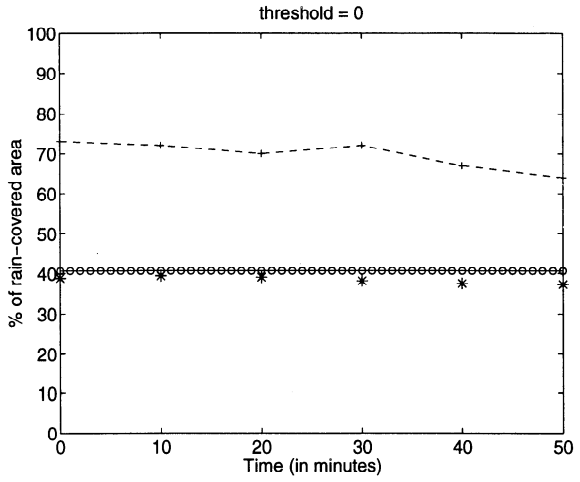

Figure 13. Storm of January 4, 1994: comparison of the percentage of rain-covered area of the predicted fields (circles) and the observed fields (asterisks), at a spatial scale of 2 km. The temporal variation of the percentage of rain-covered area at the large-scale of 32 km is also shown (dashed line). Note that the percent-area covered by rain in Figure 8 seems visually less than the actual computed values displayed above in this figure. This is because there are not enough gray-scale colors, which results in the very low rainfall intensities (of the order of 0.01 mm, the resolution of the Darwin data) being masked by zero-rainfall intensities.

is overestimated throughout the prediction time of 50 min. These same statistics are also shown in Figure 11 for a visual comparison. It is noted that the slight underestimation of $\sigma(I/I > 0)$ was not a general trend of the model and that other storms did even better than the one presented in this paper [see *Venugopal*, 1999].

Figure 12 shows the spatial correlation functions in the X direction computed from the observed and predicted fields at a spatial scale of 2 km and at times τ = 0, 10, $\cdots$, 50 min. The fields were almost isotropic, and similar results apply in the Y direction. Overall, the subgrid-scale spatial correlations are preserved well. Note that at $\tau = 0$, the 2-km predicted field was obtained from the spatial disaggregation scheme of *Perica and Foufoula-Georgiou* [1996b] and the spatial correlation structure is reproduced very well. As the initial field is evolved with the proposed dynamic-scaling-based model, some slight deviations between the spatial structure of the predicted and observed fields are noted. It is important to mention that, although, at, say, $\tau = 30$ min, applying only spatial disaggregation on the large-scale field may result in a 2-km field whose spatial correlation structure has a better resemblance to the observed field than that of Figure 12, the temporal correlation of the spatially disaggregated fields would not be as good as that of the space-time evolved fields. (This is discussed and demonstrated in greater detail later in this section; e.g., see Figure 18).

Figure 13 shows the percentage of area covered by rain as a function of time. Note that for the analyzed portion of the storm, this percentage remained almost constant over time, but this is not necessarily the case in other storms or other parts of this same storm. Comparison is made between the values obtained from the predicted and observed fields at the 2-km scale and also from the large-scale (32 km) fields. Clearly, there is definitely merit in doing downscaling, as the percentage of area above a threshold would be considerably overestimated if only the 32-km large-scale fields were used. The predicted fields compare very well with the observed fields as far as the percentage of area covered by rain is concerned. Figure 14 shows the percentage of rain-covered area above a specific threshold intensity versus the corresponding threshold intensity at two time instants, $\tau = 0$ and 50 min (similar results were found at all other instants of time). Again, the predicted fields compare very well with the observed fields throughout the storm evolution.

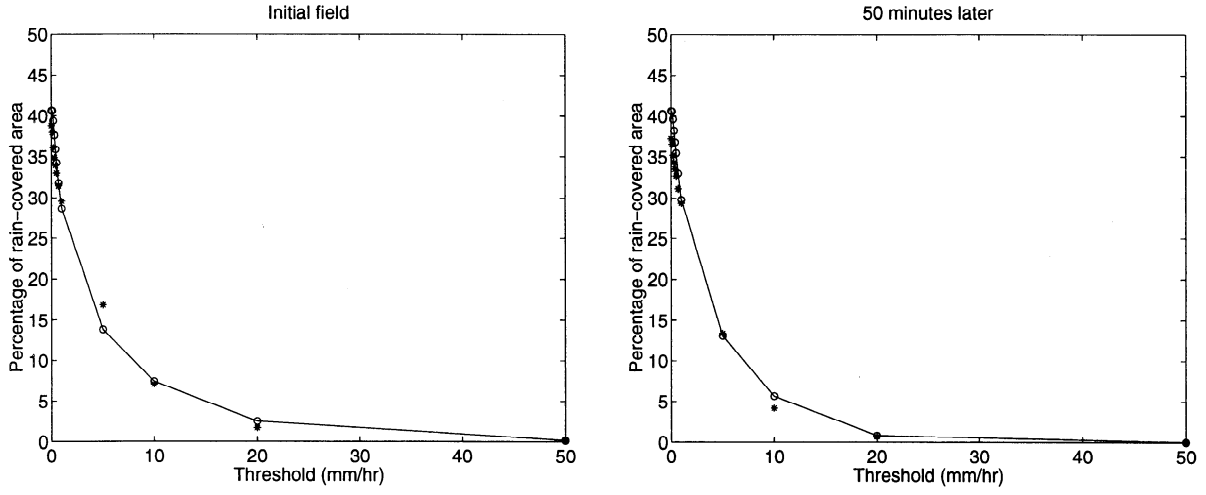

Figure 14. Storm of January 4, 1994: comparison of the variation of the percentage of rain-covered area of the predicted fields (circles) and the observed (asterisks), as a function of the corresponding threshold, at a spatial scale of 2 km and at time instants $\tau = 0$ and 50 min.

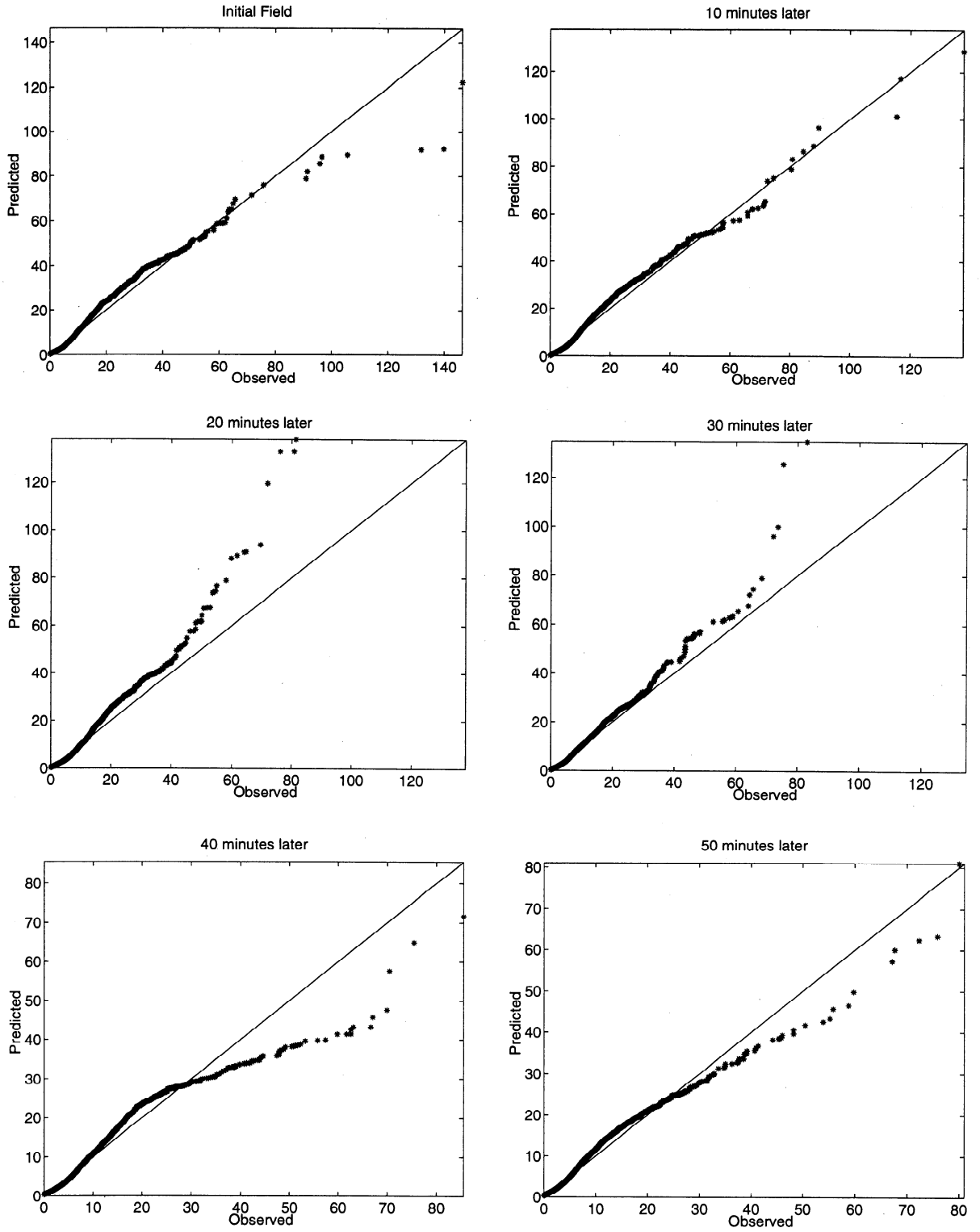

Figure 15. Storm of January 4, 1994: scattergrams of the predicted versus observed rainfall intensities (at the scale of 2 km) for the times that the observed rainfall fields were available. The values that are plotted are intensities which have been sorted in ascending order, and the "perfect correspondence line" is shown for comparison.

Another model-validation testing that was performed was by comparing scattergrams of predicted versus observed intensities. For this, intensities sorted in ascending order were plotted against each other and compared with the perfect-correspondence line. Figure 15 shows this comparison for the time instants that the observed fields were available ($\tau = 0$, 10, 20, 30, 40, and 50 min). It is evident from this figure that the body of the distribution of intensities is very well reproduced by the model (the scattergram is fitted fairly well by the 45°

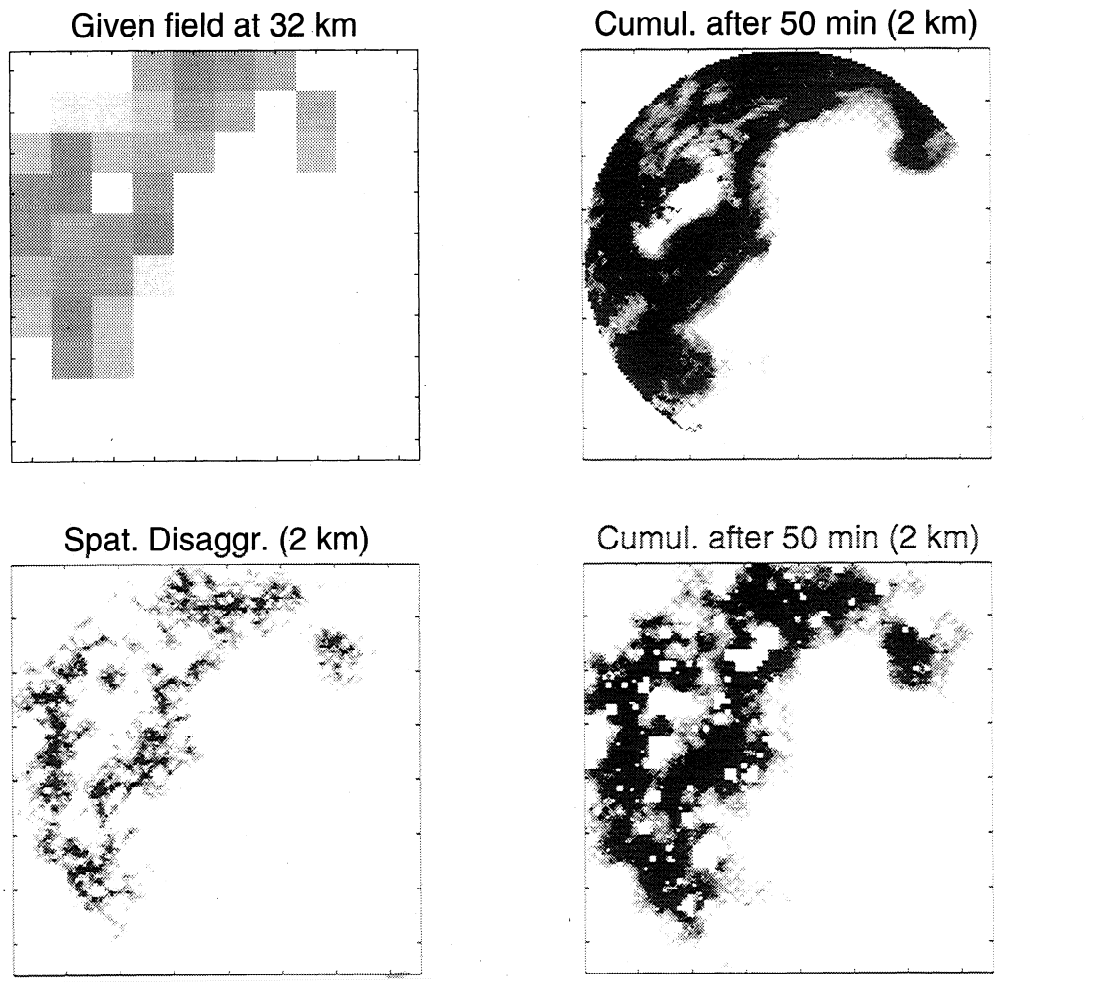

Figure 16. Storm of January 4, 1994, in Darwin, Australia. The top left panel shows the observed field at the scale of 32 km, which is the input to the downscaling model. The middle left panel shows the disaggregated field at the scale of 2 km obtained from the observed large-scale field using the spatial disaggregation scheme of *Perica and Foufoula-Georgiou* [1996b]. Validation of the proposed model is done by comparing the cumulative after 50 min, of the predicted field at the scale of 2 km obtained by the proposed space-time downscaling model (middle right panel) and the original field at the scale of 2 km (top right panel). The bottom panel shows the cumulative field after 50 min if the spatial disaggregation scheme of *Perica and Foufoula-Georgiou* [1996b] is applied to the large-scale fields every 10 min without any consideration of temporal persistence.

perfect correspondence line), but the extreme intensities are not always reproduced well and are often underestimated or overestimated. However, it is encouraging to note that the downscaling model does not seem to have a consistent trend, namely, always underestimating or overestimating the intensities, and it does not seem to deteriorate as the prediction time evolves. An upper threshold value could be applied based on the maximum observed intensities to alleviate this problem, but this was not done in this implementation.

It is noted that the development of the proposed space-time rainfall downscaling model stemmed in part from the need to correct the deficiencies that exist in using spatial disaggregation schemes to downscale from large to small scales, independently in time, without taking into account temporal persistence at subgrid scales. For that, measures evaluated from (1) the fields predicted using the proposed space-time downscaling model and (2) the fields obtained using the spatial disaggregation scheme of *Perica and Foufoula-Georgiou*

[1996b] independently in time were compared with each other and with the measures evaluated from the observed fields.

Figure 16 shows the cumulatives of the observed (top row) and predicted fields (middle row) at the scale of 2 km obtained from the proposed space-time downscaling model, after 50 min. The bottom row in Figure 16 shows the cumulative field obtained if the spatial disaggregation scheme of *Perica and Foufoula-Georgiou* [1996b] were to be applied independently in time on the large-scale fields available every 10 min. We see that this cumulative field is "smoother" than both the observed and the temporally evolved cumulative fields. This is due to the fact that temporal persistence is not incorporated here and a high value at one pixel at one time instant can be followed by a low or high value at the next time instant with an equal chance. Figure 17 shows the scattergram of the accumulated 50-min rainfall fields. Cumulative intensities, from the proposed space-time downscaling model and from the spatial disaggregation scheme, both at 2-km scale, are sorted in ascending order, and each sorted set is plotted against its counterpart from the observed fields. It is observed that the time-independent spatial disaggregation scheme does a little better than the space-time downscaling model in terms of capturing the extreme values. However, the spatially disaggregated fields lack temporal persistence and do not preserve well the temporal correlation of the observed fields at the subgrid scales.

In contrast, the newly developed space-time downscaling model results in rainfall fields which reproduce

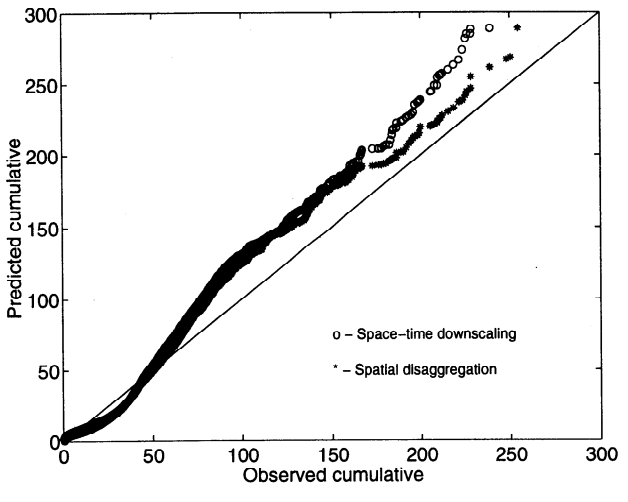

Figure 17. Storm of January 4, 1994: scattergrams of the 50-min cumulative rainfall amounts at the scale of 2 km obtained from the proposed space-time downscaling model (circles) and from the spatial disaggregation scheme of *Perica and Foufoula-Georgiou* [1996b] (asterisks), versus their counterpart from the observed fields. The values plotted are cumulatives which have been sorted in ascending order, and the perfect correspondence line is shown for comparison.

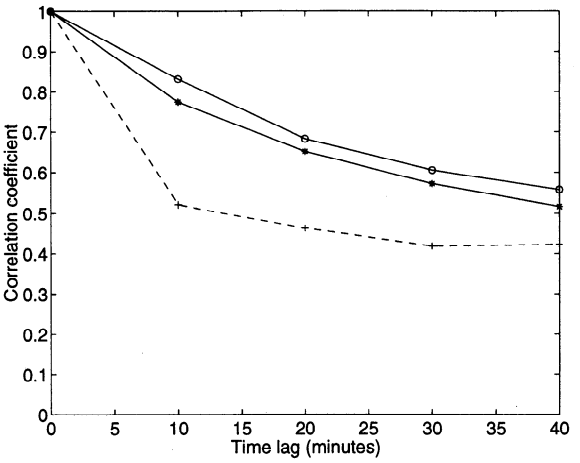

Figure 18. Storm of January 4, 1994: temporal correlations for the observed fields (asterisks), predicted fields from the proposed space-time downscaling model (circles), and fields obtained from applying the spatial disaggregation scheme (dashed line) of *Perica and Foufoula-Georgiou* [1996b] independently in time. The spatial scale of all fields is 2 km. It is evident that the proposed space-time downscaling model significantly improves the preservation of temporal persistence at the subgrid scale.

the temporal persistence of the observed fields very well. This is depicted in Figure 18 which shows the temporal correlation of the observed fields (asterisks), the predicted fields from the proposed space-time downscaling model (circles), and the fields obtained from applying the spatial disaggregation scheme independently in time (dashed line). It is evident that the independent-in-time spatially disaggregated fields decorrelate very fast while the space-time downscaled fields match well the temporal correlation of the observed fields. Preserving temporal persistence in rainfall is important in many hydrologic studies since the time history of rainfall intensities is known to affect soil-moisture storage and runoff production from a basin.

6. Conclusions

In this work, a new space-time rainfall downscaling model was proposed. The model can be used in conjunction with any spatial disaggregation scheme (here we chose to use the spatial disaggregation scheme of *Perica and Foufoula-Georgiou* [1996b]) to predict spatially evolving rainfall fields which preserve a prescribed space-time organization structure at the subgrid scales. The space-time organization has been parameterized here by dynamic scaling based on extensive evidence documented by *Venugopal et al.* [1999]. Dynamic scaling in a process implies that the evolution of the process at large space-time scales (L_1, t_1) relates to that at small space-time scales (L_2, t_2) through appropriate renormalization of space and time. The renormalization is a power law of the form $(t_1/t_2) = (L_1/L_2)^z$, where z is the dynamic scaling exponent.

The proposed model is attractive in that (1) it is parsimonious and (2) its parameterization is scale independent. In addition to capturing the spatial correlation structure of rainfall at the subgrid scale, it also has the advantage of preserving the temporal correlation structure. To apply the space-time downscaling model, one needs two parameters: H (for the spatial downscaling) and z (for the temporal evolution of the subgrid-scale fields). Estimation of the parameter H can be based on its relation to the prestorm convective available potential energy (CAPE) as proposed by *Perica and Foufoula-Georgiou* [1996a]. Estimation of the parameter z from a similar physical observable quantity has not been studied yet.

It is anticipated that z might be related to the temporal evolution of a vertical instability measure, for example, the change of CAPE over time ($d\text{CAPE}/dt$), or to parameters describing parcel buoyancy and vertical wind shear [e.g., see *Weisman and Klemp*, 1982]. However, such a study would require extensive data not typically available (for instance, radiosonde observations are sparsely available in space and time). It could well be that z can be related to the standard deviation of ΔlnI of the evolving fields. Although some preliminary evidence suggested such a possible relationship, a few cases deviated from this pattern. Analysis of more storms from different regions of the world and different climates must be done to provide insight into the variability of the parameter z and its dependence on statistical or physical parameters of the atmosphere. Also, controlled experiments, via a state-of-the-art numerical weather prediction model which can simulate high-resolution precipitation fields, together with other physically consistent parameters of the atmosphere, might provide a way of overcoming the lack-of-observations gap and at least point to possible predictive relationships which can be further verified from observations.

Acknowledgments. The material presented in this paper is based upon research supported by the GCIP program under NASA grant NAG8-1519 and partially by the NASA-TRMM program under grant NAG5-7715. The first author gratefully acknowledges support by a NASA Earth Systems Science Fellowship (NASA/NGT5-50104). We thank Robert Houze's group at the University of Washington for providing us the Darwin data. Computer resources were provided by the Minnesota Supercomputer Institute. Two anonymous reviewers made useful comments which improved the clarity of our presentation.

References

Cunning, J. B., The Oklahoma-Kansas Preliminary Regional Experiment for STORM-Central, *Bull. Am. Meteorol. Soc., 67*(12), 1478-1486, 1986.

Gupta, V., and E. Waymire, Multiscaling properties of spatial rainfall in river flow distributions, *J. Geophys. Res., 95*(D3), 1999-2009, 1990.

Kumar, P., and E. Foufoula-Georgiou, A multicomponent decomposition of spatial rainfall fields, 2, Self-similarity in fluctuations, *Water Resour. Res., 29*(8), 2533-2544, 1993.

Olsson, J., J. Niemczynowicz, and R. Berndtsson, Fractal analysis of high-resolution rainfall time series, *J. Geophys. Res., 98*(D12), 23,265-23,274, 1993.

Perica, S., and E. Foufoula-Georgiou, Linkage of scaling and thermodynamic parameters of rainfall: Results from midlatitude mesoscale convective systems, *J. Geophys. Res., 101*(D3), 7431-7448, 1996a.

Perica, S., and E. Foufoula-Georgiou, A model for multiscale disaggregation of spatial rainfall based on coupling meteorological and scaling descriptions, *J. Geophys. Res., 101*(D21), 26,347-26,361, 1996b.

Schertzer, D., and S. Lovejoy, Physical modeling and analysis of rain and clouds by anisotropic scaling multiplicative processes, *J. Geophys. Res., 92*(D8), 9693-9714, 1987.

Veneziano, D., R. L. Bras, and J. D. Niemann, Nonlinearity and self-similarity of rainfall in time and a stochastic model, *J. Geophys. Res., 101*(D21), 26,371-26,392, 1996.

Venugopal V., Spatio-temporal organization and space-time downscaling of precipitation fields, Ph.D. thesis, Univ. of Minn., Minneapolis, 1999.

Venugopal, V., E. Foufoula-Georgiou, and V. Sapozhnikov, Evidence of dynamic scaling in space-time rainfall, *J. Geophys. Res.*, in press, 1999.

Weisman, M. L., and J. B. Klemp, The dependence of numerically simulated convective storms on vertical wind shear and buoyancy, *Mon. Weather Rev., 110*, 504-520, 1982.

Wilby, R. L., and T. M. L. Wigley, Downscaling general circulation model output: A review of methods and limitations, *Prog. Phys. Geogr., 21*(4), 530-548, 1997.

Zhang, S., and E. Foufoula-Georgiou, Subgrid-scale rainfall variability and its effects on atmospheric and surface variable predictions, *J. Geophys. Res., 102*(D16) 19,559-19,573, 1997.

V. Venugopal, Center for Ocean-Land-Atmosphere Studies, 4041 Powder Mill Road, Suite 302, Calverton, MD 20705. (e-mail: venu@cola.iges.org)

Efi Foufoula-Georgiou and Victor Sapozhnikov, St. Anthony Falls Laboratory, University of Minnesota, Mississippi River at Third Avenue SE, Minneapolis, MN 55414. (e-mail: efi@mykonos.safhl.umn.edu; victor@mykonos.safhl.umn.edu)

(Received November 11, 1998; revised May 7, 1999; accepted May 17, 1999.)